

CONCRETE-TO-CONCRETE INTERFACES UNDER CYCLIC LOADING: FINITE ELEMENT ANALYSIS TOWARDS EXPERIMENTAL VERIFICATION

Vassilis K. Papanikolaou¹ and Georgia E. Thermou²

¹ Aristotle University of Thessaloniki
Civil Engineering Department
e-mail: billy@civil.auth.gr

² Aristotle University of Thessaloniki
Civil Engineering Department
gthermou@civil.auth.gr

Keywords: Concrete, Shear Transfer, Interface, Experiment, Finite elements

Abstract. *The objective of this paper is to describe a novel experimental setup for testing the concrete-to-concrete interface behavior under cyclic loading. Within the suggested configuration, various investigation parameters can be facilitated, such as the variation of concrete properties, interface roughness and number of transverse dowels. The specimen consists of three distinct concrete blocks in contact, as to create symmetric double interfaces. The middle concrete block has different concrete compressive strength, which suggests interfaces cast in different times. For the specimen preparation, elaborate computer-aided manufacturing (CAM) methods such as 3D design, laser-cutting and CNC-milling have been utilized. Moreover, an ad-hoc numerical analysis is performed, in the form of a blind-test procedure against its forthcoming experimental counterpart. The analysis is based on a three-dimensional nonlinear finite element model, accurately describing the physical specimen properties and loading setup. The analytical results are presented in a form of interface shear stress vs. slip, stress variation contours along the interface area and dowel tensile stress. A comparison with Code-based recommendations is performed and various interesting points are highlighted.*

1 INTRODUCTION

Concrete-to-concrete interfaces are formed in crack planes, construction joints, between concrete elements cast at different times and in prefabrication. Adding a new concrete layer (e.g. flexural strengthening of beams) or a new R/C member in various retrofit techniques (e.g. jacketing, infill walls) entails issues related to the connection between existing and newly cast concrete [1-3]. The response of the composite member, and subsequently of the whole structure, depends largely on the response characteristics of the interface, since shear transfer occurs.

Shear transfer along concrete interfaces is an ongoing subject of research. Many experimental test configurations have been suggested and used for studying the mechanisms that resist sliding along concrete interfaces with different characteristics (e.g. [4- 9], Fig. 1). Moreover, numerous empirical and analytical expressions have been derived for estimating the ultimate shear stress as a resultant of the various shear resistance mechanisms. A significant effort has been also made in deriving expressions describing the response of concrete-to-concrete interfaces under cyclic loading (e.g. [10, 11]). The phenomenon has also been studied numerically by finite element modeling (e.g. [12]).

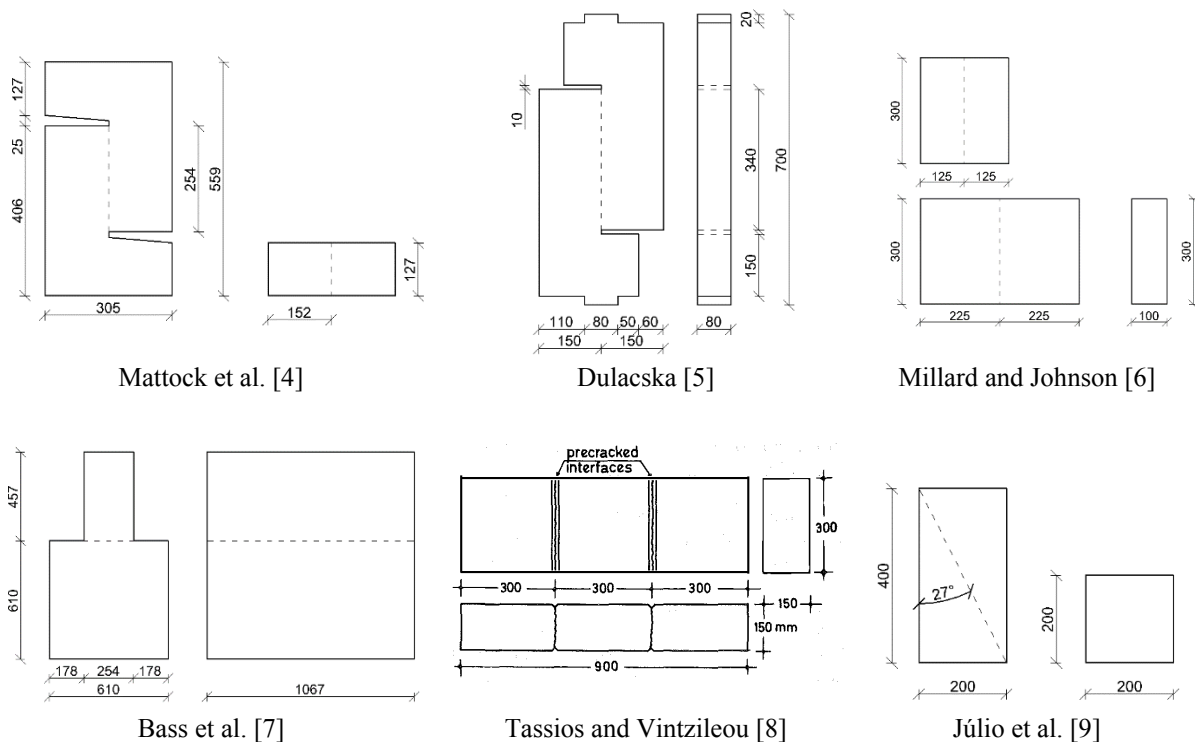


Figure 1: Different types of specimens for studying the response of concrete-to-concrete interfaces. Dimensions are given in mm [4-9].

Although the research conducted on the response of concrete-to-concrete interfaces under monotonic loading is extensive, studies referring to cyclic loading are limited. Moreover, regarding surface roughness characterization in most of the experimental studies, qualitative description relying on visual inspection is employed. This implies that the influence of roughness on the overall shear resistance is not explicitly estimated since roughness is not assessed following a quantitative procedure, as for instance the sand patch method suggested by Model Code 2010 [13]. The objective of current research is to study the shear resistance of concrete-to-concrete interfaces under cyclic loading with explicit characterization of the interface roughness. Other parameters of the experimental investigation are the concrete compressive strength

and the number of dowels perpendicularly crossing the interface. Each specimen consists of three distinct concrete blocks in contact, as to create symmetric double interfaces. The middle concrete block has different concrete compressive strength which suggests interfaces cast in different times. Before experimental testing, a finite element model of the test specimen was developed. The analytical results are presented herein in the form of interface shear stress vs slip, shear stress variation contours along the interface area and dowel tensile stresses. This analytical study is preceding, as a blind-test procedure, a consistent experimental verification, which is under preparation.

2 ESTIMATION OF SHEAR RESISTANCE ACCORDING TO CODES

Shear transfer along interfaces plays a crucial role in the response of composite members. Describing in detail the mechanisms mobilized along interfaces due to slip and their interaction is a rather complex mechanical issue, especially under cyclic loading conditions where degradation should also be accounted for. The main contributions to the overall shear resistance are described in [13]:

- Mechanical interlocking and adhesive bonding
- Friction due to external compression forces perpendicular to the interface and clamping action due to reinforcement
- Dowel action of reinforcement crossing the interface

In the following paragraphs, the expressions providing the ultimate shear resistance from codes are presented. The expressions are utilized for estimating the ultimate shear resistance of the test specimens.

Eurocode 2 [14] suggests the following expression for estimating the ultimate shear resistance at the interface between concrete cast at different times:

$$\tau_{Rd} = \underbrace{c \cdot f_{ct}}_{\text{cohesion}} + \underbrace{\mu \cdot (\sigma_n + \rho \cdot f_y)}_{\text{friction resistance}} \leq 0.5 \cdot v \cdot f_c \quad (1)$$

where:

- factor c depends on the roughness classification of the interface (very smooth: $c=0.25$, smooth: $c=0.35$, rough: $c=0.45$, indented: $c=0.50$).
- μ is the shear friction coefficient (very smooth: $\mu=0.5$, smooth: $\mu=0.6$, rough: $\mu=0.7$, indented: $\mu=0.9$).
- σ_n is the normal stress acting on the interface.
- f_{ct} is the concrete tensile stress.
- $\rho = A_s/A_c$ is the dowel reinforcement ratio.
- f_y is the steel yield stress.
- $v = 0.55 \cdot (30/f_c)^{1/3} < 0.55$ is the strength reduction factor.

Eurocode 2 [14], as it is evident from Eq. (1), does not explicitly account for the dowel action.

In Model Code 2010 [13], the shear stress developed at the interface between concrete cast at different times for interfaces intersected by dowels or reinforcement is:

$$\tau_{Rd} = \underbrace{c_r \cdot f_c^{1/3}}_{\text{cohesion}} + \underbrace{\mu \cdot (\sigma_n + \kappa_1 \cdot \rho \cdot f_y)}_{\text{friction resistance}} + \underbrace{\kappa_2 \cdot \rho \cdot \sqrt{f_y \cdot f_c}}_{\text{dowel resistance}} \leq \beta_c \cdot v \cdot f_c \quad (2)$$

The first term corresponds to the aggregate interlock and adhesive bonding where parameter c_r is modified according to the roughness of the interface [13]. The second and third term correspond to the friction and dowel resistance, respectively. Friction is related to any external compression forces normal to the interface and/or clamping forces due to reinforcement crossing the interface. In the problem examined herein, the compressive stress resulting from a normal force acting on the interface is zero ($\sigma_n = 0$). Moreover:

- ρ is the reinforcement area ratio of the reinforcing steel crossing the interface.
- f_c is the concrete compressive strength of the weakest concrete.
- f_y is the yield strength of the reinforcing bars crossing the interface
- μ is shear friction coefficient of the interface.
- κ_1 and κ_2 are interaction coefficients for tensile force activated in the reinforcement and for flexural resistance, respectively.
- β_c is the coefficient for the strength of the compression strut.
- $v = 0.55 \cdot (30/f_c)^{1/3} < 0.55$ is the strength reduction factor.

Model Code 2010 [13] relates the roughness of the interface with parameter R_t which is derived from the sand patch method. Coefficients c_r , κ_1 , κ_2 , β_c and μ receive the values presented in Table 7.3-2 of Model Code 2010 [13]. For the needs of the present study, the selected values of the coefficients c_r , κ_1 , κ_2 , β_c and μ are presented in Table 1.

Roughness	c_r	κ_1	κ_2	β_c	μ
Very smooth, $R_t = 0.0$	0	0	1.5	0.3	0.5
Rough, $R_t = 2.5$	0.1	0.5	0.9	0.5	0.7
Very rough, $R_t = 5.0$	0.2	0.5	0.9	0.5	1.0

Table 1: Coefficients for different interface roughness employed in the present study.

The ultimate shear stress of smooth interfaces according to the Greek Code for Interventions [15] is:

$$\tau_{Rd} = \underbrace{\beta_F \cdot \mu \cdot \sigma_o}_{\text{friction resistance}} + \underbrace{\beta_D \cdot \rho \cdot \sqrt{f_y \cdot f_c}}_{\text{dowel resistance}} \leq 0.3 \cdot f_c \quad (3)$$

Apart from the friction and dowel resistance, the code refers additionally to the cohesion resistance (a value equal to $0.25 \cdot f_{ct}$ is suggested for smooth interfaces, where f_{ct} is the tensile stress of the weakest concrete) and states that it should be ignored in the presence of clamping action of reinforcing bars crossing the interface. Moreover, it is mentioned that in case of smooth interfaces the contribution of the clamping action is low and could be ignored. From the above, the dowel resistance is considered the only mechanism that resists sliding at the interface. The terms β_F and β_D are participation factors of the friction and dowel resistance, respectively, taken both equal to 0.5. In case of rough interfaces, Eq. (2) is further modified to:

$$\tau_{Rd} = \underbrace{\beta_F \cdot \mu \cdot \left[f_c^2 (\sigma_c + \rho \cdot f_y) \right]^{1/3}}_{\text{friction resistance}} + \underbrace{\beta_D \cdot \rho \cdot \sqrt{f_y \cdot f_c}}_{\text{dowel resistance}} \leq 0.3 \cdot f_c \quad (4)$$

The first term of Eq. (4) represents the contribution of concrete as it depends on the frictional resistance of the interface planes.

The shear strength of an interface where reinforcement is placed perpendicular to the shear plane is estimated according to ACI 318-14 [16]:

$$\tau_{Rd} = \mu \cdot \rho \cdot f_y \quad (5)$$

where $\rho = A_s/A_c$ is the area ratio of the shear-friction reinforcement, f_y is the yield strength of reinforcing bars and μ is the friction coefficient, which for normal weight concrete may range between 0.6 for concrete placed against hardened concrete that is clean and not intentionally roughened and 1.4 for concrete placed monolithically. ACI-318-14 [16] provides upper limits on shear friction strength. In case of normal weight concrete placed monolithically or placed against hardened concrete intentionally roughened the maximum shear strength is calculated as:

$$\tau_{Rd} = \min(0.2f_c, 3.3 + 0.2f_c, 11) \text{ in MPa} \quad (6)$$

For all the above cases (Eqs. 1-6), the ultimate shear force transferred along the interface is estimated by:

$$V_{Rd} = \tau_{Rd} \cdot A_c \quad (7)$$

where A_c is the area of the interface.

3 DESIGN OF EXPERIMENTAL SETUP

The main concept behind the suggested experimental setup is to test concrete-to-concrete interfaces under pure shear, minimizing any adverse normal-to-interface actions caused by loading or geometric, first or second-order eccentricities (see Fig. 2). These normal actions could considerably affect the interface response, since they may induce additional friction stresses ($\mu \cdot \sigma$) along the interface plane. Consequently, a symmetric double-interface solution was followed (as in [8]), as depicted in Fig. 2.

Specifically, the specimen is consisted of three adjacent 250×250×400 mm concrete blocks, with the central one representing concrete cast at an earlier time (old) and the other two at present (new), allowing different old/new concrete strength configurations, as per the ordinary repair/strengthening practice (e.g. R/C jacketing). Between old and new concrete, two symmetrically arranged interfaces are formed, which effective area is deliberately reduced to 150×300 mm by applying a 50 mm wide, thin insulating material on the perimeter (e.g. clear tape), before casting new concrete. The purpose of the above reduction is twofold, i.e. to localize failure on the interface by avoiding possible edge splitting cracks and to reduce the interface shear resistance to manageable levels. Both interfaces are crossed by a configurable number (2, 4, 6, 8 or 10) of 8 mm diameter (Ø8), 500 mm length dowels. These dowels are arranged on a 60×50 mm, five-row by two-column grid and they are anchored at a length of 125 mm inside the new concrete block, complying with minimum Code requirements [15]. Cyclic loading is vertically applied on the middle block by fixing the two adjacent ones, creating symmetric stress flow to the two centerline-equidistant interface planes. For mounting purposes, four plastic tubes are longitudinally inserted in each block (Ø32 and Ø20 for old and new, respectively), allowing the insertion of threaded rods after casting, which will be subsequently anchored to the testing apparatus (described later). Finally, four Ø8 closed hoops are also inserted in each block, providing a minimum level of confinement.

In order to realize the above elaborate specimen configuration, a special steel mold was designed and manufactured with the aid of 3D software. The main requirements for the design were the ability to facilitate different casting phases (old and new concrete), different dowel configurations and interface roughness, while providing a convenient and fast assembly/disassembly process. Fig. 3 (left) shows the various parts of the steel mold that were laser-cut from a 5 mm thick steel plate. It is based on a modular male-to-female connection concept, assisted by interlocking side bars. Various circular openings can accommodate precise dowel and tube

positioning as well as necessary uplifting handles. The molds were manufactured and assembled in the Laboratory of R/C and Masonry Structures, Civil Engineering Dept., Aristotle Univ. of Thessaloniki, Greece.

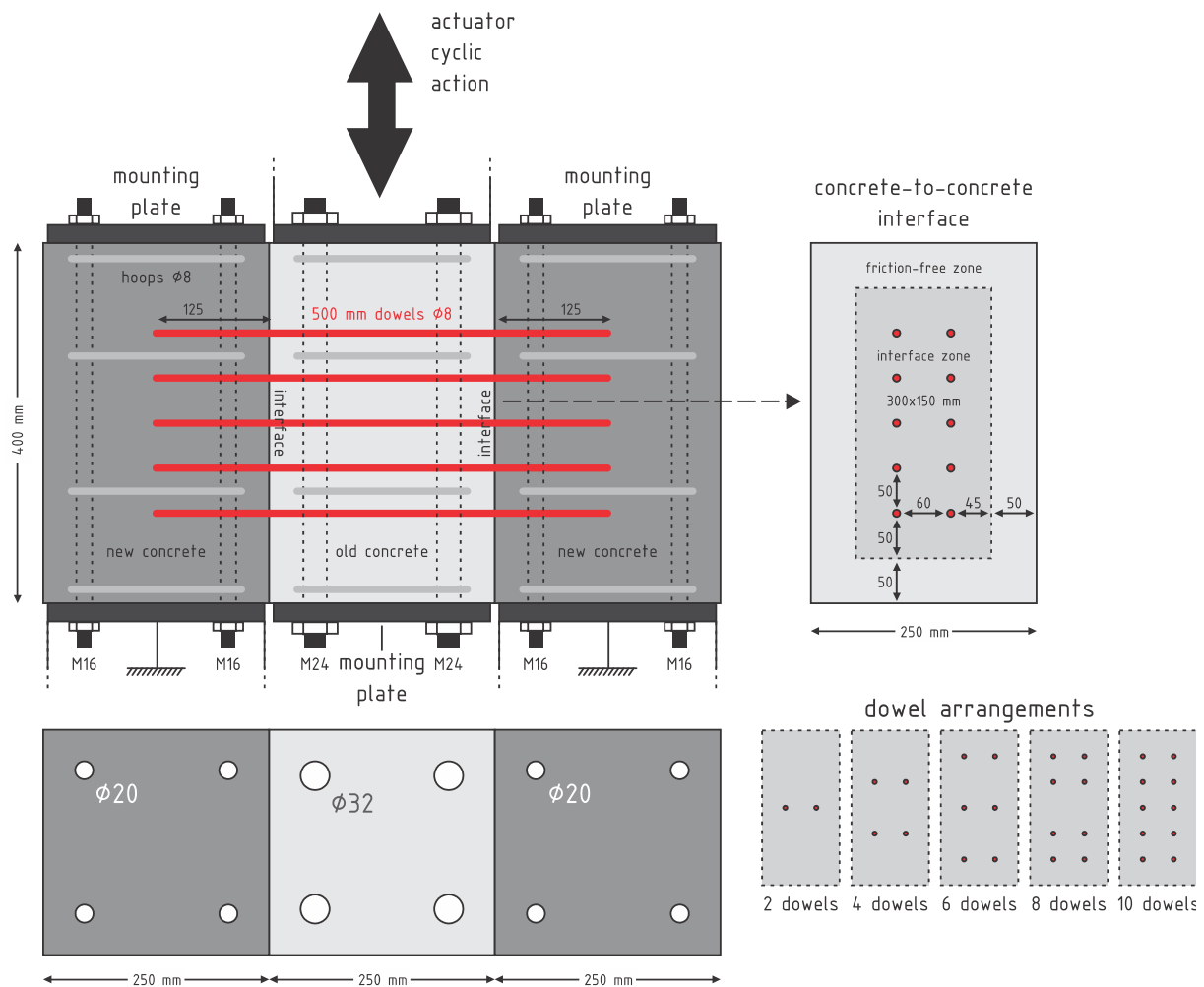


Figure 2: Specimen design concept.

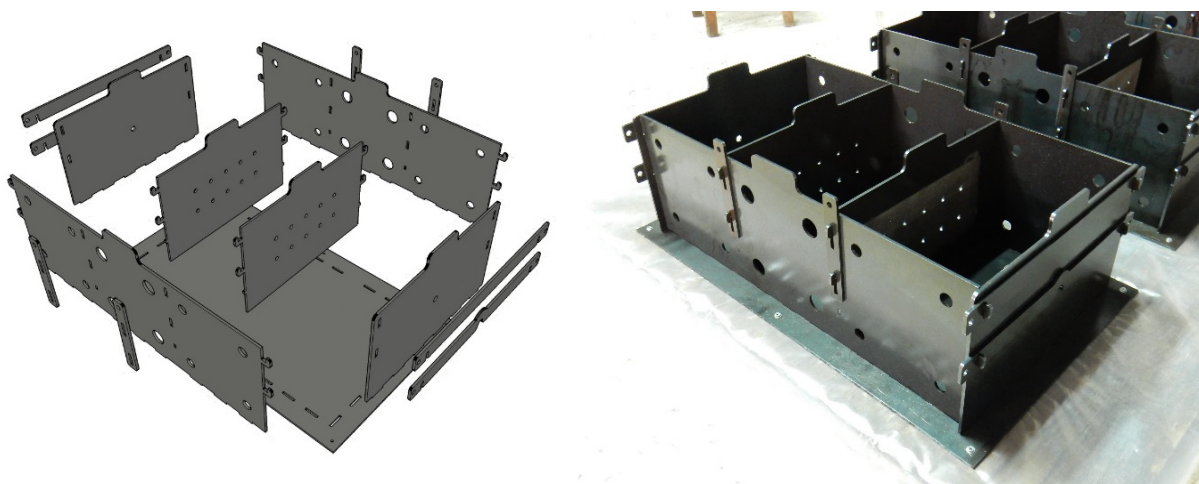


Figure 3: Casting mold design and assembly.

The two middle panels which separate the old from new concrete blocks are removable and can be positioned with either face against the central block. When removed (after casting and curing of the central block), they naturally form a very smooth, effectively zero-roughness surface. However, for investigating the effect of different interface roughness, three middle panel pairs were subsequently machined (on one face), in order to ‘stamp’ a pattern of prescribed roughness against the central block. These patterns were produced by precise CNC cross-routing using a 90° included angle bit, covering the aforementioned 150×300 interface zone (Fig. 4). The milling depth (h) and spacing (s) were calculated for yielding exact values of the roughness parameter (R_t), according to the sand patch method [13] (Eq. 8, Table 2). Three different roughness values, $R_t = 2.5$, 5.0 and 10.0 were selected, corresponding to rough, very rough and extremely rough conditions (for the rest smooth panel faces, it is assumed that $R_t = 0.0$).

$$R_t = \frac{40 \cdot V_{\text{sand}}}{\pi \cdot d^2} = \frac{40 \cdot \frac{V_{\text{pyramid}}}{V_{\text{parallelogram}}} \cdot V_{\text{cylinder}}}{\pi \cdot d^2} = \frac{40 \cdot \frac{V_{\text{pyramid}}}{V_{\text{parallelogram}}} \cdot \frac{\pi \cdot d^2}{4} \cdot h}{\pi \cdot d^2} = 10 \cdot \frac{V_{\text{pyramid}}}{V_{\text{parallelogram}}} \cdot h \quad (8)$$

R - Rough		VR - Very rough		ER - Extremely rough	
h (mm)	0.5	h (mm)	1.0	h (mm)	2.0
s (mm)	1.6	s (mm)	3.2	s (mm)	6.4
b (mm)	0.6	b (mm)	1.2	b (mm)	2.4
$V_{\text{pyr.}} / V_{\text{par.}}$	0.505	$V_{\text{pyr.}} / V_{\text{par.}}$	0.505	$V_{\text{pyr.}} / V_{\text{par.}}$	0.505
R_t	2.53	R_t	5.05	R_t	10.10

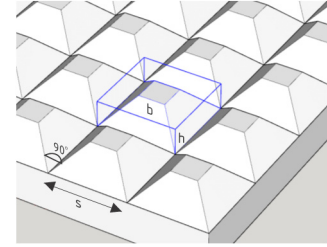


Table 2: Calculation of prescribed roughness.

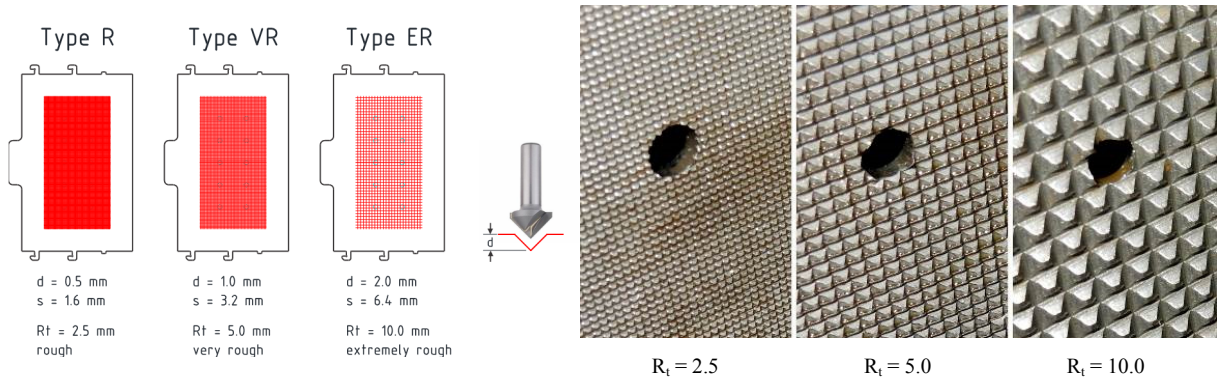


Figure 4: Prescribed roughness configurations.

The specimen preparation using the above steel mold can be easily accommodated in nine steps, as follows (Fig. 5):

- Step 1:* Assemble the central chamber by positioning both middle panel faces according to the required interface roughness ($R_t = 0.0$, 2.5, 5.0 or 10.0). Lock middle panels.
- Step 2:* Insert the four Ø32 tubes and the four Ø8 hoops in the central chamber.
- Step 3:* Insert the required number of dowels (2, 4, 6, 8, or 10), taping the rest of the holes (if any).
- Step 4:* Cast the central concrete block (old).
- Step 5:* After curing of the central block, unlock and remove the two middle panels.

Step 6: Insert and lock the two end panels, insert Ø20 tubes and hoops in the empty chambers and position the two lifting bars (Ø12).

Step 7: Cast the new concrete.

Step 8: After curing, disassemble mold completely.

Step 9: Cut tubes flush, lift and rotate specimen for mounting on the loading apparatus.

The finalized specimen is positioned and mounted on the loading apparatus, as depicted in Fig. 6. The two end blocks are firmly mounted on the two vertical pedestals using eight M16 threaded rods and two 20 mm thick steel plates, placed on the top of the blocks. The middle block is mounted on a hydraulic actuator via a swivel appendage (extender), four M24 threaded rods and a 20 mm thick steel plate, placed on the bottom of the block. This configuration allows the actuator to transfer a prescribed cyclic action to the middle block by applying concentric compressive pressure only, either directly (downward movement) or through the bottom plate, by tensioning the four embedded rods (upward movement). The apparatus base is secured via two M36 threaded rods on the laboratory floor, featuring a 1.0×1.0 m grid of 80 mm diameter holes. The critical loading capacity of the apparatus is determined by the yielding strength of the eight M16 rods (722 kN, considering 8.8 material grade and 10% pre-tension), after providing a large safety margin against welding failure.

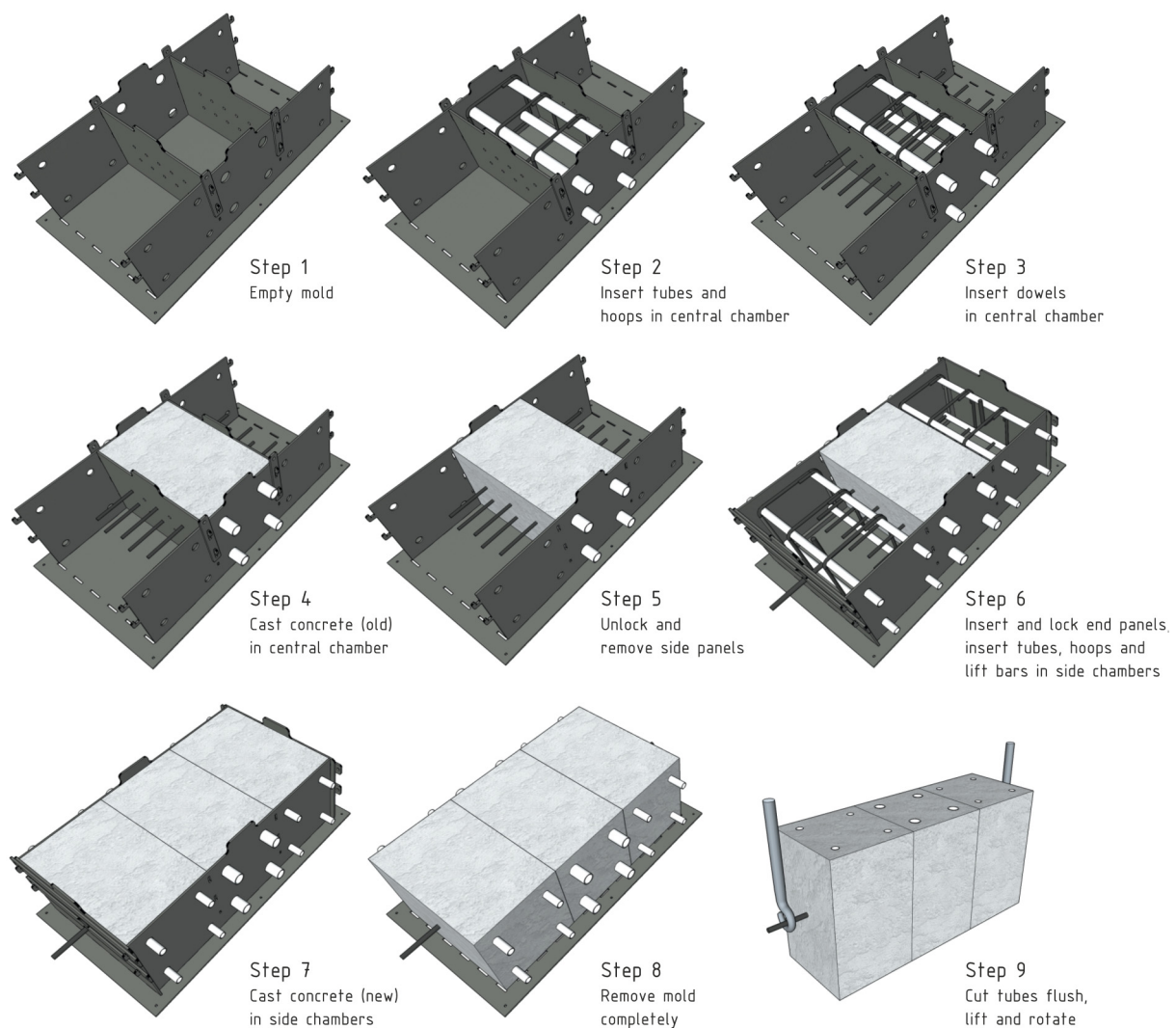


Figure 5: Specimen casting procedure.

A prescribed displacement cyclic load history will be imposed by a single-ended hydraulic actuator (MTS 243.60) mounted on a steel loading frame, with a load capacity of 1013 kN (compression) / 648 kN (tension) and a full stroke of ± 250 mm. The actuator is equipped with a build-in LVDT device for measuring the imposed displacements. However, since both the loading frame and the apparatus is naturally susceptible to (elastic) bending during specimen loading (especially for large loads), additional displacements could be picked up by the actuator internal LVDT, resulting to a discrepancy between the desired (target) displacement load history and the measured displacement of the internal LVDT. This adverse effect may become critical in the present setup, since the applied displacements will be in the order of a few millimeters. For this reason, the actuator closed-loop control will be transferred from the default actuator internal LVDT to an external measurement system, based on a draw-wire sensor (or alternatively a short-stroke LVDT), mounted on the transverse beam between two vertical pedestals and connected to the bottom face of the mounting plate (Fig. 6). The above experimental setup is currently under preparation and will be utilized shortly.

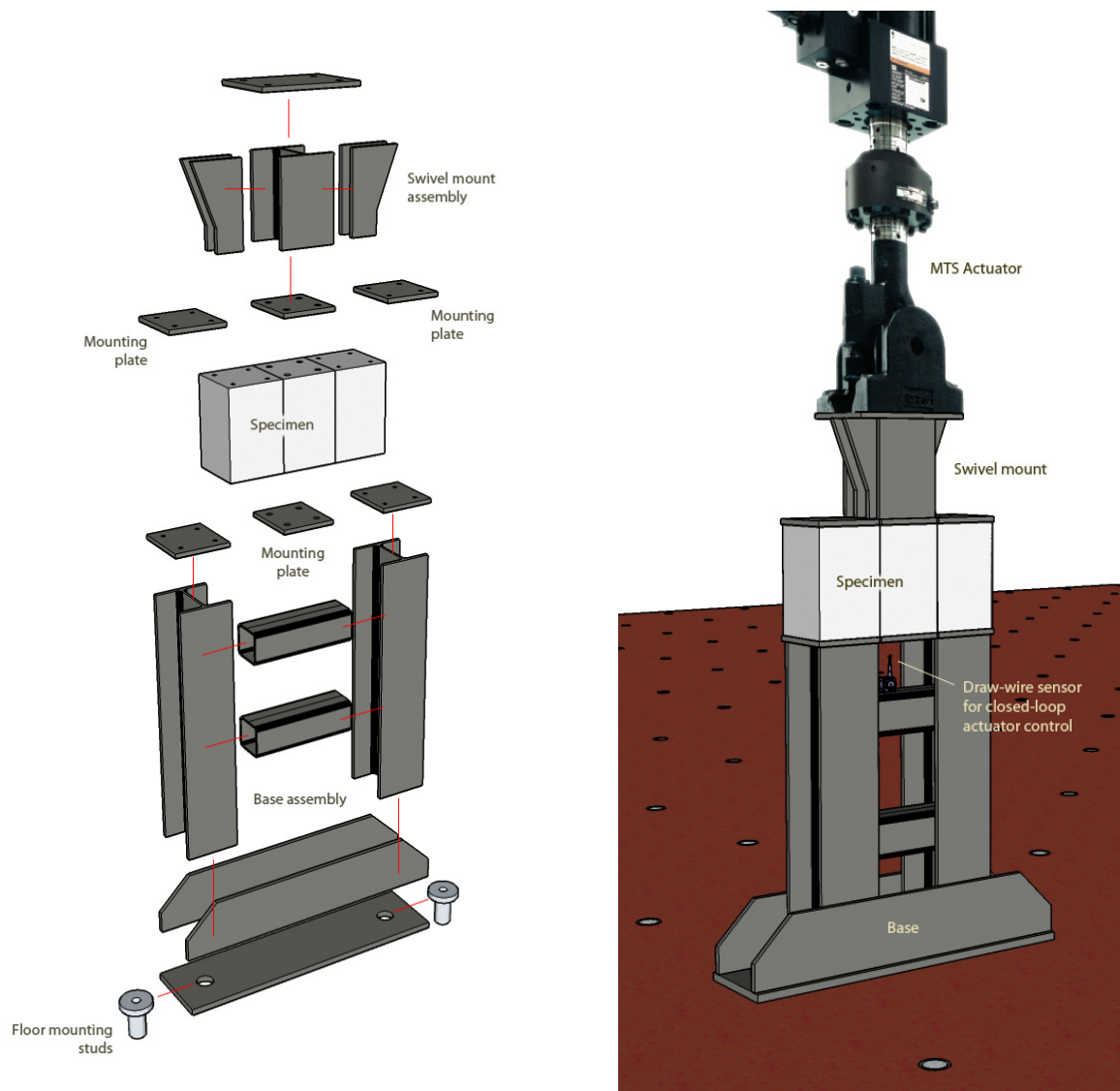


Figure 6: Testing apparatus design, assembly and configuration.

4 NUMERICAL ANALYSIS AND RESULTS

Before conducting experimental testing, an ad-hoc numerical analysis has been performed, serving as a blind-test prediction against its forthcoming experimental counterpart. The analysis is based on a three-dimensional nonlinear finite element model using the ATENA software [17], accurately describing the physical specimen properties and loading setup, as depicted in Fig. 7. For the old and new concrete blocks, the mean compressive and tensile strength properties of C12 and C20 concrete classes were employed, respectively [13, 14], assigned to a nonlinear fracture-plastic concrete constitutive model. Loading was applied in the form of prescribed displacement, via a rigid loading block on the top of the middle concrete block, as per the experimental setup. The top and bottom sides of the two adjacent blocks were fixed. The common planes (contacts) between old and new concrete were divided to the inner interface zone and the friction-free zone (see Fig. 2), assigned to a Mohr-Coulomb interface model and a no-contact formulation, respectively. The dowel reinforcement was modeled using a batch of eight reinforcement fibers for each Ø8 bar (each having an equivalent area of $50.3/8 \text{ mm}^2$ and a yield strength of $f_y = 500 \text{ MPa}$). This technique was preferred instead of the standard reinforcement representation using a single axial-only truss element, so that the bending action is modeled as well. The dowel bond-slip behavior was also accounted for, using a Code based constitutive model for pullout action and good bond conditions [13]. The global mesh size was fixed to $2.5 \times 2.5 \text{ cm}$, however, for increased accuracy, the mesh density was increased to 0.5 cm , in both normal directions to each interface zone, for a length of 5 cm . The model parameters analyzed were the number of dowels (2, 4 and 6) as well as the interface roughness, corresponding to smooth, rough and very rough conditions ($R_t = 0.0, 2.5, 5.0$). The corresponding friction (μ) and cohesion (c) values for the employed Mohr-Coulomb model were taken equal to $\mu = 0.5, 0.7, 1.0$ and $c = c_r \cdot f_c^{1/3} = 0.0, 0.27, 0.54 \text{ MPa}$, respectively (Table 1, [13]).

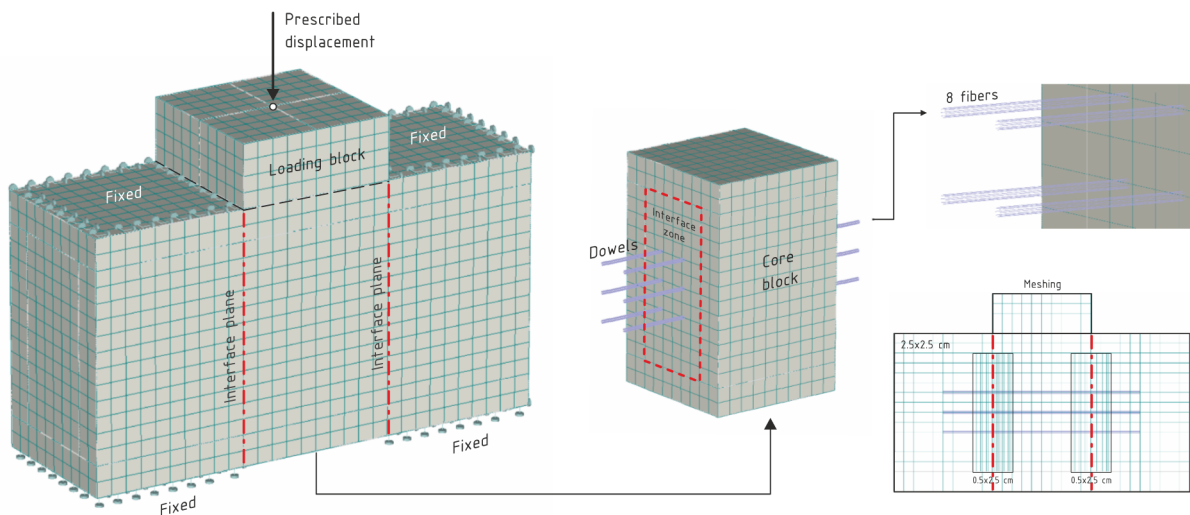


Figure 7: Finite element model details.

The analysis results in terms of total shear force (reaction at the point of prescribed displacement) vs interface slip are shown in Fig. 8. It is observed that the interface shear resistance is clearly increased for an increasing number of transverse dowels, as expected. A similar increase in shear resistance for rougher interfaces is not evident, however, increased roughness yields lower values of interface slip at maximum shear, indicating a stiffer interface response. Moreover, it is observed by comparing against a perfect-bond analysis that the effect of dowel bond-slip plays a predominant role in determining the interface stiffness, leading to a considerably

stiffer response if neglected. By comparing the shear resistance of the various interface configurations between the present analysis and the various code recommendations (Eqs. 1-6, Fig. 9), a large dispersion in the results is observed, especially for different interface roughness levels. This implies that the friction contribution on the interface resistance is an issue that needs further investigation especially in cyclic loading conditions.

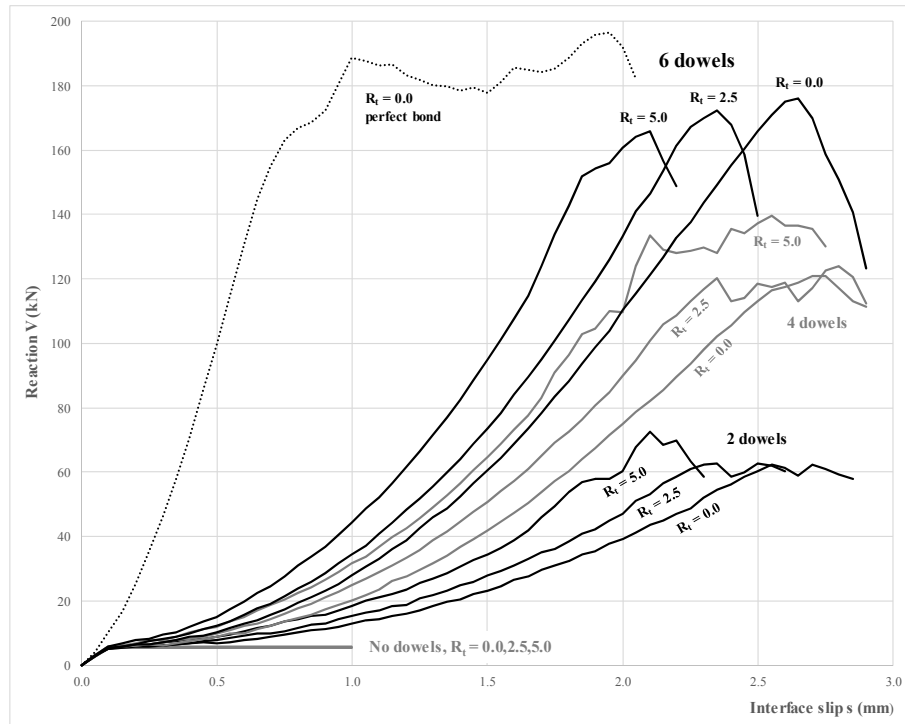


Figure 8: Interface response from finite element analysis.

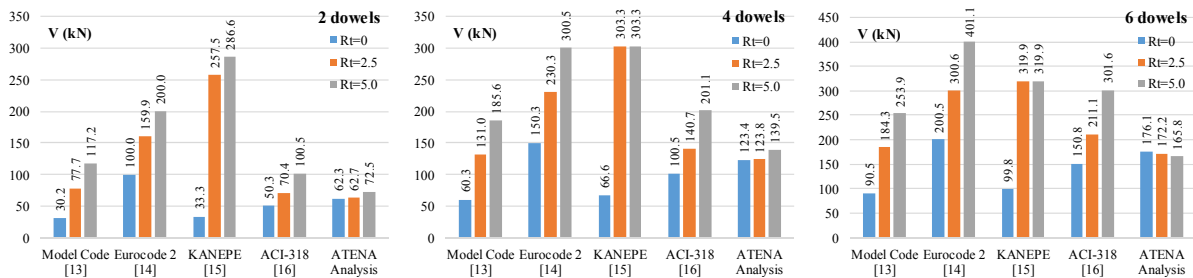


Figure 9: Comparison between analysis and various Code recommendations.

As far as the above friction contribution issue is concerned, all Code recommendations suggest that the total shear stress, which includes a significant friction component (depending on the stress normal to the interface), is uniform throughout the whole interface area (Eq. 7). However, from the analysis stress contours at maximum force (Fig. 10), it is observed that the normal stress produced by the dowel clamping action that creates friction (σ_{xx}) is operating only on a limited ellipsoidal boundary around dowels, while the remaining interface area is practically unstressed (red color), hence inducing no friction resistance. This is also visible in the stress distribution parallel to the interface (σ_{zz}), where unstressed regions are greatly influential. Pending experimental verification, this question is herein raised for further discussion.

In Fig. 11, the dowel deformed shape (10× magnification) and the tensile stress contours at maximum shear force are depicted. It is observed that dowel yielding ($\sigma_c = f_y = 500$ MPa) occurs

at the vicinity of the interface planes as expected, and that a gradual stress degradation is formed along the dowel length (reaching zero at both ends) due to the consideration of the bond-slip effect. Finally, the fiber division technique applied for dowel bars successfully captured their bending action, i.e. stress non-uniformity across the dowel section depth.

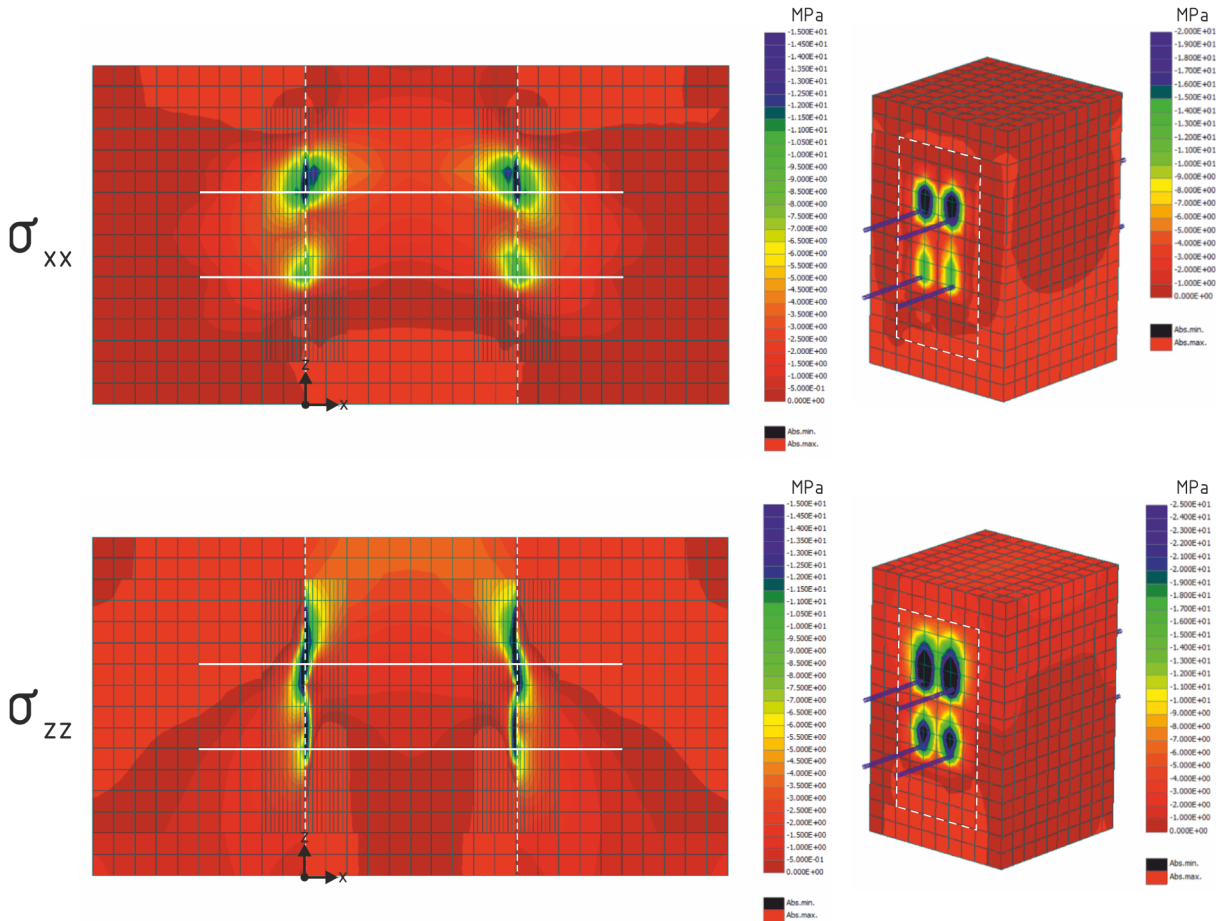


Figure 10: Cross-interface longitudinal and transverse stress contours at max shear force (4 dowels, $R_t = 5.0$)

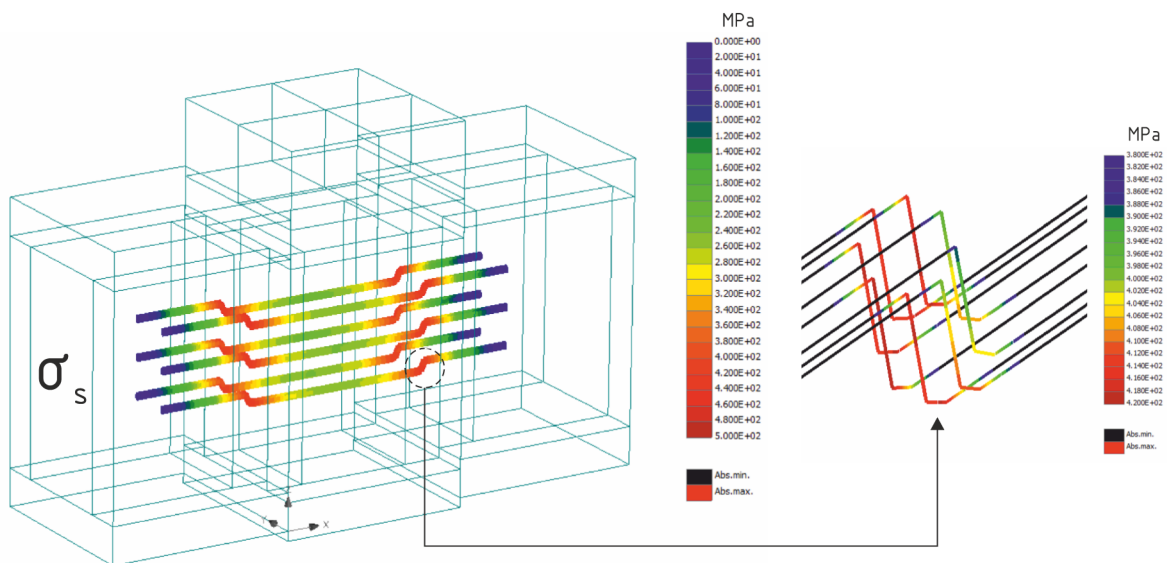


Figure 11: Dowel stresses and deformations at max shear force (6 dowels, $R_t = 0.0$)

5 CONCLUSIONS

In this paper, a novel experimental setup for testing the concrete-to-concrete interface behavior in various configurations under cyclic loading was described. The main concept was to create interfaces under pure shear which resulted in a symmetric double-interface solution, thus minimizing any adverse normal actions due to eccentricities. The parameters to be investigated is the number of transverse dowels and interface roughness, which for the first time is prescribed using elaborate CAM methods. While the suggested setup is under preparation, an ad-hoc non-linear finite element analysis was performed, serving as a preceding blind test procedure to be compared with forthcoming experimental results. The analysis results showed acceptable correlation in terms of interface shear resistance compared to various Code recommendations, which however show a significant scatter, especially for larger interface roughness levels. This may be accounted to the fact that under pure shear, friction is mobilized on a limited boundary around dowel positions. Moreover, the complete force vs slip curves provided by the finite element model gives a clearer view in terms of interface stiffness, where both roughness and dowel bond-slip play a significant role. Notwithstanding, the actual experimental testing is expected to further clarify the above issues and provide better overall insight on the present complex research topic.

ACKNOWLEDGEMENTS

The present research is funded by the program “Supporting new researchers in lecturer position”, Research Committee, Aristotle University of Thessaloniki, Greece. The first author would also like to thank D. Orfanidis, MSc and TECHNOMETAL for the technological support.

REFERENCES

- [1] G.E. Thermou, S.J. Pantazopoulou, A.S. Elnashai, Flexural behavior of brittle R/C members rehabilitated with concrete jacketing. *Journal of Structural Engineering*, ASCE, **133**(10), 1373-1384, 2007.
- [2] G.E. Thermou, V.K. Papanikolaou, A.J. Kappos, Flexural behaviour of reinforced concrete jacketed columns under reversed cyclic loading. *Engineering Structures*, **76**, 270-282, 2014.
- [3] G.E. Thermou, Strengthened Structural Members and Structures: Analytical Assessment, *Encyclopedia of Earthquake Engineering*, edited by Michael Beer, Edoardo Patelli, Ioannis Kouglioumtzoglou and Ivan Siu-Kui Au, www.SpringerReference.com (invited article), 2014.
- [4] A. Mattock, W. Li, T. Wang, Shear transfer in lightweight reinforced concrete. *PCI Journal*, **21**(1), 20-39, 1976.
- [5] H. Dulacska, Dowel action of reinforcement crossing cracks in concrete. *ACI Journal*, **69**, 754-757, 1972.
- [6] S.G. Millard, R.P. Johnson, Shear transfer across cracks in reinforced concrete due to aggregate interlock and to dowel action. *Magazine of Concrete Research*, **36**(126), 9-21, 1984.

- [7] R.A. Bass, R.L. Carasquillo, J.O. Jirsa, Shear transfer across new and existing reinforced concrete. *ACI Structural Journal*, **86(4)**, 383-393, 1989.
- [8] T.P. Tassios, E.N. Vintzileou, Concrete-to-concrete friction, *ASCE Journal of Structural Engineering*, **113(4)**, 832-849, 1987.
- [9] E.N.B. Júlio, F.A. Branco, V.D. Silva, Concrete-to-concrete bond strength. Influence of the roughness of the substrate surface. *Construction and Building Materials*, **18(9)**, 675-681, 2004.
- [10] I. Vassilopoulou, T.P. Tassios, Shear transfer capacity along a R/C crack under cyclic sliding. *Proceedings of the fib Symposium*, **271**, Technical Chamber of Greece, Athens, Greece, 2003.
- [11] V. Palieraki, E. Vintzileou, C. Zeris, Behaviour of interfaces in repaired/strengthened R/C elements subjected to cyclic actions: Experiments and Modelling. *3rd International Symposium on life-cycle and sustainability of civil infrastructure systems (IALCCE'12)*, Vienna, Austria, 2012.
- [12] D. Dias-da-Costa, J. Alfaiate, E.N.B. Júlio, FE modeling of the interfacial behaviour of composite concrete members, *Construction and Building Materials*, **26(1)**, 233-243, 2012.
- [13] fib [Fédération Internationale du Béton], Model Code 2010 Vol. 1 & 2, Bulletin No. 65 & 66, 2013.
- [14] CEN [European Committee for Standardization], Eurocode 2. Design of concrete structures – Part 1–1: General rules and rules for buildings (EN 1992-1-1). Brussels, 2004.
- [15] EPPO [Earthquake Planning and Protection Organization], Greek Code for Interventions (KANEPE), Athens, 2013.
- [16] ACI Committee 318 318-14, Building Code Requirements for Structural Concrete (ACI318-02) and Commentary ACI 318 R-02. Detroit, 2014.
- [17] V. Červenka, L. Jendele, J. Červenka, ATENA Program Documentation. Part 1: Theory, Červenka Consulting, Prague, Czech Republic, 2015.